Vacancy-Induced Magnetism in ZnO Thin Films and Nanowires

doi: 10.1103/PhysRevB.77.205411

Vacancy-induced magnetism in ZnO thin films and nanowires

Qian Wang,[1,2] Qiang Sun,[3,4,2,*] Gang Chen,[2] Yoshiyuki Kawazoe,[5] and Puru Jena[2]
[1]*School of Physical Science and Technology, Southwest University, Chongqing 40071, People's Republic of China*
[2]*Department of Physics, Virginia Commonwealth University, Richmond, Virginia 23284, USA*
[3]*Department of Advanced Materials and Nanotechnology, Peking University, Beijing, People's Republic of China*
[4]*Center for Applied Physics and Technology, Peking University, Beijing, People's Republic of China*
[5]*Institute for Materials Research, Tohoku University, Sendai 980-8577, Japan*
(Received 5 January 2008; revised manuscript received 8 April 2008; published 9 May 2008)

Extensive calculations based on density functional theory have been carried out to understand the origin of magnetism in undoped ZnO thin films as found in recent experiments. The observed magnetism is confirmed to be due to Zn, instead of O, vacancy. The main source of the magnetic moment, however, arises from the unpaired $2p$ electrons at O sites surrounding the Zn vacancy with each nearest-neighbor O atom carrying a magnetic moment ranging from 0.490 to 0.740 μ_B. Moreover, the study of vacancy-vacancy interactions indicates that in the ground state, the magnetic moments induced by Zn vacancies prefer to ferromagnetically couple with the antiferromagnetic state lying 44 meV higher in energy. Since this is larger than the thermal energy at room temperature, the ferromagnetic state can be stable against thermal fluctuations. Calculations and discussions are also extended to ZnO nanowires that have larger surface to volume ratio. Here, the Zn vacancies are found to lead to the ferromagnetic state too. The present theoretical study not only demonstrates that ZnO samples can be magnetic even without transition-metal doping but also suggests that introducing Zn vacancy is a natural and an effective way to fabricate magnetic ZnO nanostructures. In addition, vacancy mediated magnetic ZnO nanostructures may have certain advantages over transition-metal doped systems in biomedical applications.

DOI: 10.1103/PhysRevB.77.205411 PACS number(s): 75.70.−i

I. INTRODUCTION

Currently, ZnO-based materials have been receiving considerable attention due to their potential applications in spintronics, light-emitting diodes, laser diodes, UV detectors, cosmetics, and biomaterials. The attractive properties of ZnO include (1) large exciton binding energy (60 meV) that allows efficient excitonic lasing at room temperature, (2) piezoelectricity enabling high electromechanical coupling, (3) capability to be grown at low temperature even on a plastic substrate, and (4) large electronegativity of oxygen leading to strong p-d exchange coupling between band carriers and localized spins. The novel magnetic, electronic, optical, and electromechanical properties of ZnO offer the unique possibility to multifunctionally create integrated devices for sensing, processing, and actuating functions in one monolithic structure. However, one of the main obstacles in realizing the full potential of ZnO materials is lack of a full understanding of the role of intrinsic and extrinsic lattice defects, which largely affect the electronic and optical properties. For example, the origin of magnetism of transition-metal doped ZnO[1] is poorly understood and there are debates whether this is caused by defects other than the metal dopants. Several types of defects, such as oxygen vacancy,[2–4] zinc interstitial,[5,6] hydrogen interstitial,[7,8] zinc vacancy,[9,10] as well as oxygen interstitial,[11] have been reported, which attract extensive research interest.[12,13]

Recently, some experiments have reported that one of the main species of defects detected by positron annihilation spectroscopy is Zn vacancy in both ZnO thin films[9,10,14,15] and bulk samples.[16] More interestingly, a recent experiment reported that Zn vacancy induces ferromagnetism in undoped ZnO thin films, where the magnetization depends on thickness of the thin films.[17] Thus, an essential question arises: How do Zn vacancies induce magnetism in ZnO thin films?

Due to the covalent bonding features in ZnO, the physics of defects in ZnO is quite complex, and the understanding of the nature of defects is challenging. No explanation exists to account for the reason why Zn vacancy could cause ferromagnetism in undoped ZnO thin films. Similarly, one does not know how the magnetic moments are distributed around the Zn vacancy. It is also important to know whether Zn vacancies prefer to occupy the surface, subsurface, or bulk sites. Do they like to cluster or remain isolated? If they do cluster, is the magnetic coupling affected? Does the observed ferromagnetism originate from surface Zn vacancies? If so, ZnO nanowires would also exhibit ferromagnetism because of its large surface to volume ratio.

II. COMPUTATIONAL METHOD

In this paper, we present the first comprehensive theoretical investigation that addresses above questions. The theoretical calculations are carried out by using density functional theory[18] that incorporates exchange and correlation effects within the generalized gradient approximation (GGA).[19] We have used the PW91 functional[20] for GGA and a plane-wave basis set with the projector augmented wave method[21] as implemented in the Vienna *ab initio* simulation package (VASP).[22] The cutoff energy was set at 350 eV for the plane-wave basis (the default of maximum cutoff energy is 276.75 eV). In all calculations, self-consistency was achieved with a tolerance in the total energy of at least 1 meV. Hellman–Feynman force components on each ion in

the supercells are converged to 1 meV/Å. The accuracy of our calculations for ZnO system has been well established from our previous work.[23,24] The calculated unit cell lattice parameters, $a=b=3.262$ Å and $c=5.226$ Å, are in good agreement with experimental results within the average error of ~1%.

The formation energy of a point defect in neutral state is calculated[25] by using the following equation:

$$E_f = (E_{\text{tot}}^d - E_{\text{tot}}^0 + n_i\mu_i)/n_i, \quad (1)$$

where E_{tot}^d is the total energy of the supercell containing the defects, E_{tot}^0 is the total energy of the corresponding perfect supercell, n_i is the number of atoms removed, and μ_i is chemical potential of the corresponding atom. The chemical potential μ_i depends on the experimental growth conditions. In thermodynamic equilibrium, the Zn and O chemical potentials must satisfy the stability condition for ZnO, namely,

$$\mu_{\text{Zn}} + \mu_{\text{O}} = \Delta H(\text{ZnO}). \quad (2)$$

Here, ΔH is the formation enthalpy of ZnO, which is determined from the computed total energies of wurtzite ZnO, hexagonal close-packed Zn, and molecular O_2. The calculated formation enthalpy of ZnO is −3.42 eV, which is comparable with the experimental value of −3.6 eV.[26] The extreme O-rich condition is given by the energy of O in an O_2 molecule. The extreme Zn-rich condition is given by the energy of Zn in bulk zinc ($\mu_{\text{Zn}}=E_{\text{tot}}^{\text{Zn}}$), which corresponds to the lower limit of O-poor condition. The range of ambient O from O poor to O rich is subject to the magnitude of the formation enthalpy of ZnO.

III. RESULTS AND DISCUSSION

A. Vacancy-induced magnetism in ZnO thin films

We first study the effect of O and Zn vacancies on the electronic properties and magnetism of ZnO thin films. The ZnO thin film was modeled by a (2×2) seven-layer slab having $[11\bar{2}0]$ surface orientation (see Fig. 1), which contains a total of 56 f.u of ZnO. Each slab was separated from the other by a vacuum region of 10 Å along the $[11\bar{2}0]$ direction. The central three layers of the slab were held at their bulk position, while the two layers on either side of the slab were taken to be identical to preserve symmetry and allowed to relax without any symmetry constraint. The surface reconstruction was carried out by optimizing geometry of the supercell by using a $5\times5\times1$ Monkhorst–Pack k-point mesh.[27] The relaxation energy per surface Zn-O dimer is found to be 0.215 eV. The relaxed Zn-O bond length on the surface layer along the [0001] direction is 1.888 Å, which corresponds to a contraction of −5.2% from the bulk value. The Zn-O bond length approximately along the $[1\bar{1}00]$ changes from 1.973 to 1.901 Å, which corresponds to a contraction of −3.6%. The calculated results are in good agreement with our previous work for the (1×2) slab supercell, in which the thickness of the slab with seven layers and the vacuum space with 10 Å have been verified to be adequate for studying the effects of surface.[23] The total electronic densities of states (DOSs) for spin-up and spin-down electrons that correspond to the pure ZnO $(11\bar{2}0)$ thin film supercell are plotted in Fig. 2 (a_1). We note that the curves of DOS for spin-up and spin-down states are totally symmetric, and the Fermi level is located in the gap region, suggesting that ZnO $(11\bar{2}0)$ thin film is a semiconductor and nonmagnetic.

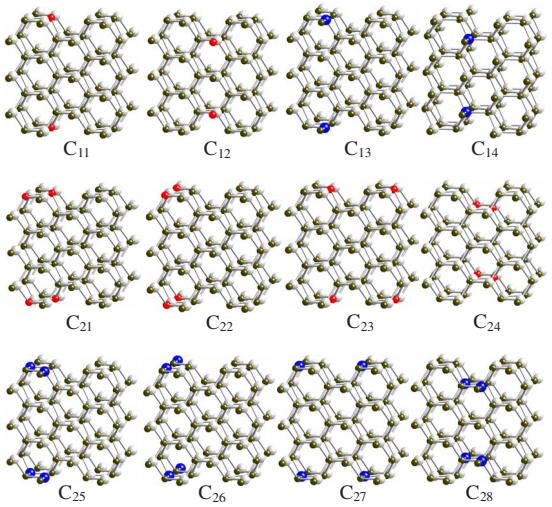

FIG. 1. (Color online) Schematic representation of the nonequivalent vacancy configurations in $Zn_{56}O_{56}$ supercell modeling ZnO $(11\bar{2}0)$ thin film. The darker spheres represent O atoms, the lighter spheres represent Zn atoms, and the red and blue spheres correspond to O and Zn vacancies, respectively.

We created an O vacancy by removing a *single* O atom from the surface layer of the slab. To preserve the symmetry, the O atom on opposite side of the slab was also removed, as shown in Fig. 1 (C_{11}). This led to a $Zn_{56}O_{54}$ supercell with O vacancy concentration of 3.6%. The total energy calculation and the geometry optimization for this configuration were carried out by using a $5\times5\times1$ Monkhorst–Pack grid. The formation energy is found to be 3.179 eV/O vacancy, but no magnetism appears in the system. To see if O vacancy prefers to lie on a subsurface site, we removed an O atom from the subsurface layer on either side of the slab, as shown in configuration C_{12} in Fig. 1. The corresponding formation energy is found to increase to 3.791 eV, which is comparable to the calculated value of 3.72 eV for O vacancy in ZnO bulk.[25] Thus, it is clear that formation of an O vacancy on the surface layer is easier than that in the subsurface layer or in the bulk. More importantly, ZnO with O vacancy is nonmagnetic irrespective of where the O vacancy lies.

Next, we generated a Zn vacancy by removing a single Zn atom on each side of the surface and subsurface layers in the supercell. These are, respectively, labeled as configurations C_{13} and C_{14} in Fig. 1. The formation energies of Zn vacancy for configurations C_{13} and C_{14} are 5.377 and 5.988 eV, respectively. Note that like O vacancy, Zn vacancy prefers to be on the surface. We should note that the large formation energies for both Zn and O vacancies are due to strong covalent Zn-O bonds and the surface vacancies are easier to form because there is less number of bonds that need to be broken on the surface than in the subsurface.

Unlike the system with O vacancies, ZnO containing Zn vacancies is magnetic. The calculated total magnetic mo-

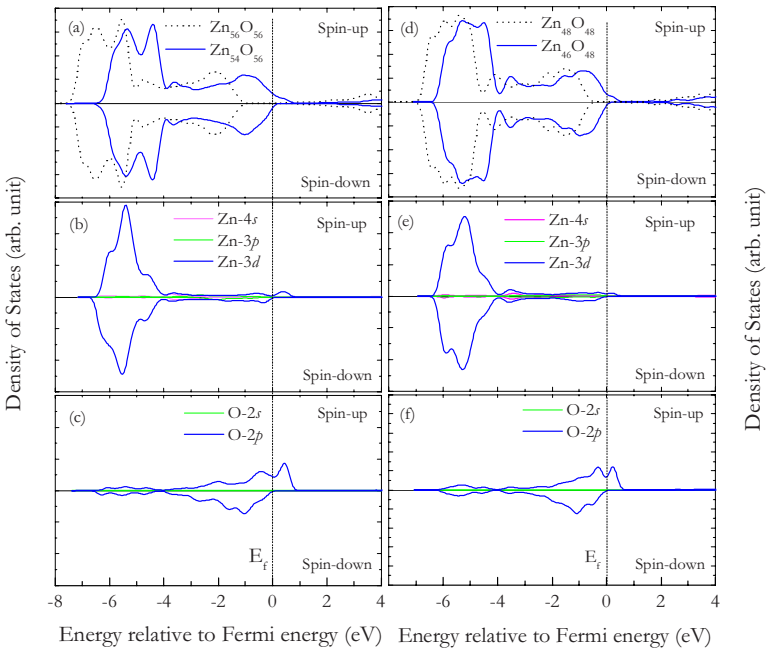

FIG. 2. (Color online) (a) Total DOS, (b) partial DOS of Zn atom, and (c) partial DOS of O atom in the $(11\bar{2}0)$ thin film $Zn_{56-x}O_{56}$ ($x=0$ and 2) supercell. (d) Total DOS and partial DOS of (e) Zn and (f) O atoms in the nanowire $Zn_{48-x}O_{48}$ ($x=0$ and 2) supercell.

ments for configurations C_{13} and C_{14} are 3.091 and 2.196 μ_B, respectively, which imply that one Zn vacancy on the surface of ZnO thin film can induce a moment of up to 1.504 μ_B. To further examine the origin and distribution of this moment, we calculated the magnetic moment on each O and Zn atom self-consistently for all of the configurations as well as the charge-density distribution for configuration C_{13} with and without Zn vacancy. The latter are plotted in Figs. 3(a) and 3(b), respectively. We see that no significant amount of charge is left at the vacancy site. The main contribution to the magnetic moment comes from the three O atoms that are nearest neighbor to the Zn vacancy. On the $(11\bar{2}0)$ thin film surface, each Zn atom directly binds with three O atoms, in which two of them are on the surface layer while the third one resides in the subsurface layer. The two surface O atoms [labeled O_1 and O_2 in Fig. 3(b)] have magnetic moments of 0.480 and 0.385 μ_B, respectively. These mainly arise from the O $2p$ orbitals (0.478 and 0.383 μ_B). The O atom in the subsurface layer has a moment of 0.116 μ_B with 0.114 μ_B resulting from O $2p$ orbitals. The Zn atoms nearest to the Zn vacancy on the surface layer, i.e., Zn_1 and Zn_2 in Fig. 3(b), contribute only 0.033 and 0.024 μ_B, respectively, to the magnetic moment, which are negligible. In configuration C_{14}, although the total moment introduced by Zn vacancy is smaller (2.196 μ_B) than that in configuration C_{13} (3.091 μ_B), the moment distribution has similar feature, i.e., the moments mainly come from the O atoms nearest to the Zn vacancy. The O atom on the surface layer has the largest local moment, namely, 0.335 μ_B. The other two O atoms on the second layer only carry magnetic moments of 0.172 and 0.170 μ_B, and the one in the third layer has a magnetic moment of only 0.060 μ_B. The calculated results are in good agreement with recent experiment in which the magnetization of very thin films was found to be much larger than that of the thicker films,[17] suggesting that the Zn vacancies are mostly located on the surface.

To visualize the changes in electronic structure and magnetic properties resulting from Zn vacancies, we plot the total DOS corresponding to configuration C_{13} in Fig. 2. This shows that Zn vacancy induces spin polarization of the top of the valence band. We note that there is a significant change in the spin-up and spin-down total DOS at the Fermi level in $Zn_{54}O_{56}$ compared to that in nonmagnetic pure ZnO. The energy gap disappears and the Zn vacancies introduce new states near the Fermi level resulting in an asymmetric spin-up and spin-down DOSs. To understand the origin of this change, we calculated the partial DOS at Zn_1 and O_1 sites in Fig. 3(b), which are the nearest neighbors to the Zn vacancy. These are plotted in Figs. 2(b) and 2(c), respectively. They show that there is no visible contribution to the observed magnetism from the Zn atom. On the other hand, the main contribution to the moment comes from the O $2p$ orbitals. The spins of O $2p$ electrons are polarized and introduce new states near the Fermi level. Thus, it is clear that in ZnO thin film, the presence of Zn vacancies leads to the spin polarization of O $2p$ orbitals in the gap region and magnetism does not result from Zn $3d$ orbitals. This confirms the experimental suggestion that the observed ferromagnetism arises not from O vacancies but from Zn vacancies.[17] Although the formation energy of Zn vacancy is higher than that of O vacancy, both Zn and O vacancies can be generated during the growth and deposition process because of thermal fluctuation or growth conditions, as found in experiments.[9,10,14,15,17]

To study the effect of vacancy concentration on ferromagnetism in the undoped ZnO thin film with Zn vacancy, we generated two O and two Zn vacancies, respectively, on either side of the slab with different vacancy distances. This corresponds to 7.14% O and Zn vacancy concentration, respectively. The vacancy configurations are schematically pictured in Fig. 1 [(C_{21})–(C_{28})]. The geometries were fully relaxed and the total energies were calculated using the same procedure as described above. The calculated results are listed in Table I.

The formation energies per O vacancy are found to be 3.304, 3.215, 3.203, and 3.820 eV for configurations

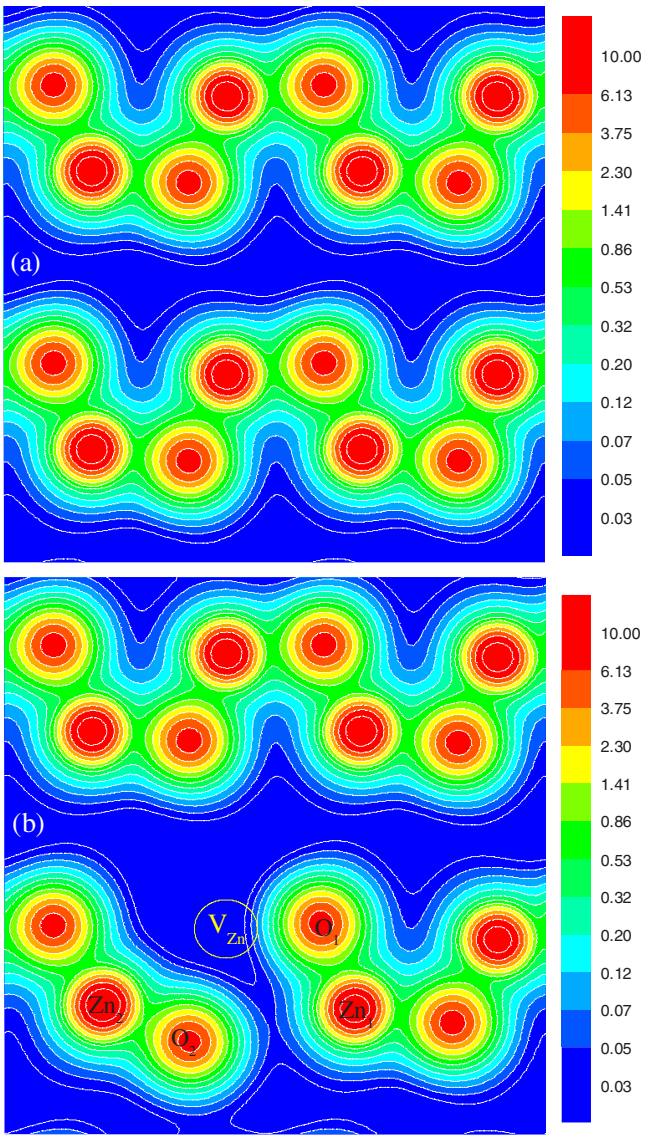

FIG. 3. (Color online) Two-dimensional distribution of charge density on the surface of the $(11\bar{2}0)$ plane for both (a) $Zn_{56}O_{56}$ and (b) $Zn_{55}O_{56}$ supercells.

$C_{21}-C_{24}$, respectively, which indicates again that O vacancies prefer to be on the surface. In addition, the O vacancies do not prefer to cluster as configuration C_{23} where the distance between two vacancies is 5.68 Å is lower in energy by 0.403 eV than configuration C_{21}. None of the configurations, $C_{21}-C_{24}$, exhibit magnetism, suggesting that O vacancies will not lead to magnetism in ZnO even if the vacancy concentration is increased.

On the other hand, we found that the system exhibits magnetism with a total magnetic moment of 6.478–6.970 μ_B when the ZnO thin film contains a 7.14% Zn vacancy (see Fig. 1 and Table I). We note that a higher Zn vacancy concentration introduces a larger total moment in the system. The moments at the nearest neighboring O atom of the vacancy are found to be 0.737, 0.742, 0.510, and 0.604 μ_B for configurations $C_{25}-C_{28}$, respectively. The formation energies of Zn vacancy range from 5.12 to 6.04 eV.

TABLE I. Formation energy E_f (in eV) of the vacancy, total magnetic moment M_{tot} (in μ_B) per supercell, and local magnetic moment M_{local} (in μ_B) at the nearest-neighbor O site in $Zn_{56}O_{52}$ and $Zn_{52}O_{56}$ supercells (see Fig. 1).

Configuration	E_f	M_{tot}	M_{local}
C_{21} (V_O)	3.304	0.000	0.000
C_{22} (V_O)	3.215	0.000	0.000
C_{23} (V_O)	3.203	0.000	0.000
C_{24} (V_O)	3.820	0.000	0.000
C_{25} (V_{Zn})	5.120	6.542	0.737
C_{26} (V_{Zn})	5.177	6.478	0.742
C_{27} (V_{Zn})	5.387	6.970	0.510
C_{28} (V_{Zn})	6.036	6.581	0.604

It is interesting to note that, unlike O vacancies, Zn vacancies prefer to cluster and reside on the surface of ZnO thin film. The ground state configuration is found to be C_{25} that is, respectively, 0.260, 1.068, and 3.662 eV lower in energy than the other three configurations, C_{26}, C_{27}, and C_{28}. This is associated with the bond length contraction of the atoms around the vacancies and is caused by the large surface reconstruction when the two Zn vacancies are close to each other. For instance, the bond length of ZnO along the [0001] direction contracted from 1.888 to 1.830 Å around the vacancies. Clustering Zn vacancies found here is consistent with recent experiment[16] where Zn vacancy clusters of up to five missing Zn-O pairs have been observed.

To further understand the onset of ferromagnetism observed in the recent experiment,[17] we study the stability of the ferromagnetic (FM) state vs antiferromagnetic (AFM) state and the coupling between the two Zn vacancies. The energy difference between the FM and AFM couplings of the two Zn vacancies (V_{Zn_1} and V_{Zn_2}), which is defined as $\Delta E^{\text{mag}}(V_{Zn_1}\text{-}V_{Zn_2}) = E(V_{Zn_1}\uparrow V_{Zn_2}\downarrow) - E(V_{Zn_1}\uparrow V_{Zn_2}\uparrow)$ is calculated. The results are plotted in Fig. 4. The symbol $V_{Zn}\uparrow$ stands for spin-up state, where the spins at O sites nearest to the Zn vacancy are up. $V_{Zn}\downarrow$ corresponds to the analogous spin-down state. For ground state configuration C_{25} (see Fig. 1), it was found that the FM state is 44 meV lower in energy than the AFM state. For the other two higher energy configurations of C_{26} and C_{27}, the energy differences ΔE^{mag} were found to be 35 and 33 meV, respectively, which are larger than the thermal energy that corresponds to the room temperature. Therefore, the FM state could be stable against thermal fluctuation. This is in agreement with the experimentally observed ferromagnetism[17] in undoped ZnO thin film induced by Zn vacancy.

B. Vacancy-induced magnetism in ZnO nanowires

To study the effect of surface curvature on the magnetic properties of ZnO, we have carried out calculations on nanowires. We constructed a ZnO nanowire from a $(7\times7\times2)$ ZnO bulk supercell having wurtzite structure by removing zinc and oxygen atoms from the outside area of the circle in Fig. 5(a) and replacing with a vacuum space. The nanowire

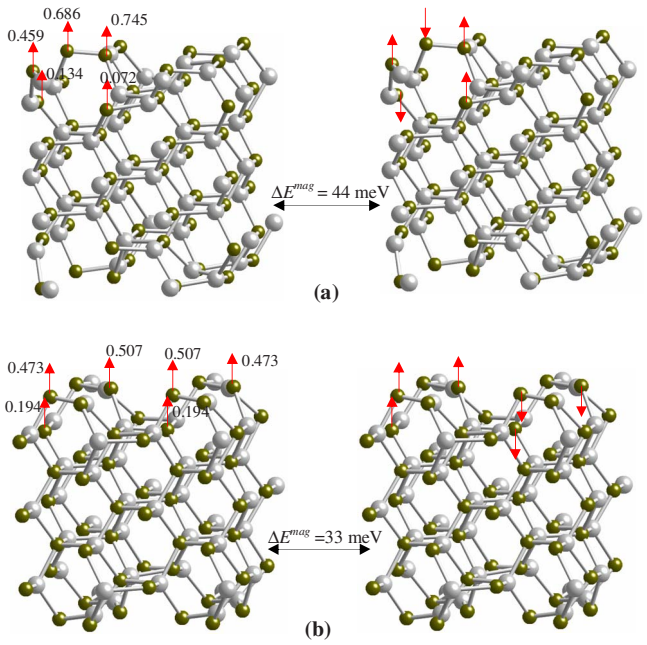

FIG. 4. (Color online) The spin alignments and the magnetic moments (in μ_B) of the nearest-neighbor O sites to the Zn vacancies in configurations (a) C_{25} and (b) C_{27}, respectively.

supercell thus created contains 48 f.u. of ZnO with a vacuum space of 12.997 and 13.011 Å along the $[10\bar{1}0]$ and $[01\bar{1}0]$ directions, respectively. The wire extends to infinity along the [0001] direction through repetition of the periodic supercell [see Fig. 5(b)].

To study the properties of O and Zn vacancies in the nanowire, we first created an O and Zn vacancy on the surface sites marked by red and blue spheres in Fig. 6 (a_1) and (b_1), respectively. O and Zn vacancies created inside the

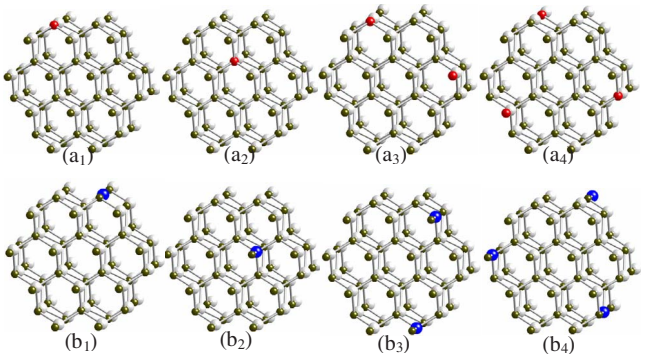

FIG. 6. (Color online) The schematic representation of the nonequivalent vacancy configurations in $Zn_{48-x}O_{48-y}$ nanowire supercell. The darker and lighter spheres represent O and Zn atoms, respectively. The red and blue spheres show the sites where the atoms are removed to generate O and Zn vacancies, respectively.

nanowire are shown in Fig. 6 (a_2) and (b_2), respectively. The later calculations are carried out to investigate the preferred sites of the vacancies. We then removed two and three O and Zn atoms in the supercell, respectively [see Fig. 6 (a_3), (a_4), (b_3), and (b_4)], to study the influence of vacancy concentration on the magnetic properties of the nanowire.

Total energy calculations with full geometry optimization were carried out for all the configurations of $Zn_{48-x}O_{48-y}$ (x =0, 1, 2, and 3 and y=0, 1, 2, and 3, respectively) in Fig. 6 by using a $5\times5\times1$ Monkhorst–Pack k-point mesh.[27] The calculated results are summarized in Table II. Calculations were also carried out for supercell $Zn_{48}O_{48}$ without any vacancy. It was found that the relaxation of the atomic positions is significant due to the large surface area. For instance, in perfect ZnO crystal, the calculated Zn-O bond length along the [0001] direction is 1.993 Å and that between Zn and the three nearest O atoms in (0001) plane is 1.975 Å.

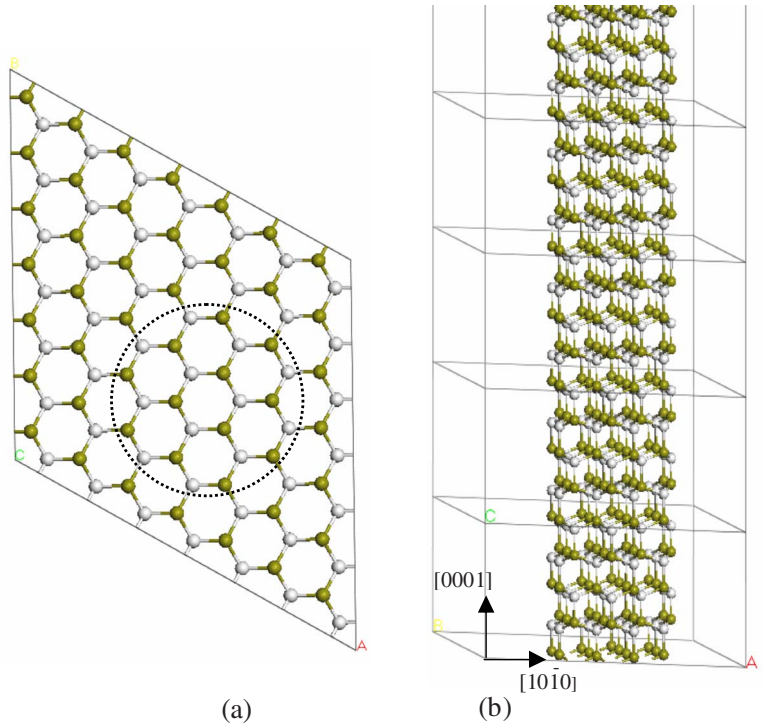

FIG. 5. (Color online) (a) Top view of a $7\times7\times2$ ZnO supercell (0001) plane having wurtzite structure. (b) A ZnO nanowire supercell ($Zn_{48}O_{48}$) which extends to infinite along the [0001] direction.

TABLE II. Formation energy E_f (in eV) of the vacancies, total magnetic moment M_{tot} (in μ_B) per supercell, and local magnetic moment M_{local} (in μ_B) on the nearest-neighbor O site for different vacancy concentrations and configurations (see Fig. 6) for $Zn_{48-x}O_{48-y}$ nanowire supercell.

Configurations	E_f	M_{tot}	M_{local}
(a_1) (V_O at 2.08%)	3.051	0.000	0.000
(a_2) (V_O at 2.08%)	3.907	0.000	0.000
(a_3) (V_O at 4.17%)	3.058	0.000	0.000
(a_4) (V_O at 6.35%)	3.139	0.000	0.000
(b_1) (V_{Zn} at 2.08%)	5.149	1.546	0.492
(b_2) (V_{Zn} at 2.08%)	5.318	0.000	0.000
(b_3) (V_{Zn} at 4.17%)	5.173	3.216	0.510
(b_4) (V_{Zn} at 6.35%)	5.310	4.954	0.604

The Zn-O bond length changed to 1.888 Å for the surface atoms in the [0001] direction and to 1.956 Å between the surface and subsurface layer atoms in the (0001) plane of the $Zn_{48}O_{48}$ supercell. The electronic structure of the nanowire can be seen from the total DOS in Fig. 2(d), where the spin-up and spin-down DOSs are totally symmetric and the energy gap is located around the Fermi level. Thus, the system is nonmagnetic and semiconducting.

The calculated O and Zn vacancy formation energies on the nanowire surface are, respectively, 3.051 and 5.149 eV, while those inside of the nanowire are 3.907 and 5.318 eV. This indicates that the energy cost to remove an O atom is much less than that for a Zn atom in the nanowire, and both O and Zn vacancies prefer to reside on the nanowire surface. These features are the same as that found in the thin film. However the vacancy formation energies for O and Zn on the nanowire are less than those for corresponding configurations (C_{11}–C_{14}) in the thin film, demonstrating that vacancies can more easily form in nanowires than in thin films. It was also found that $Zn_{47}O_{48}$ supercell carries a total moment of 1.55 μ_B, while the total moment for $Zn_{48}O_{47}$ is calculated to be 0 μ_B. This shows that O vacancy does not introduce any magnetism in the nanowire system in spite of its curved surface. We also found that the nanowire remains nonmagnetic even though the O vacancy concentration is increased to 6.35%.

For Zn vacancy, however, the situation is different. The total magnetic moment changes from 1.546 μ_B to 4.954 μ_B when the concentration increases from 2.08% to 6.35%. On the contrary, the vacancy formation energy changes only by 0.06 eV. Thus, nanowires provide the added advantage that the magnetic moments can be increased by increasing the Zn vacancy concentration without significant energy cost. It is also found that the moment is contributed from the neighboring O atoms of the vacancy. The local moments on the nearest-neighbor O site are 0.510 and 0.604 μ_B and mainly arise from the from O $2p$ orbitals (0.507 and 0.602 μ_B). From the calculated results for configuration (b_2) in Fig. 6 (see Table II), we note that the formation energy for Zn vacancy inside of the nanowire is higher than that on the surface and these Zn vacancies inside do not lead to magnetism because of the stronger orbital hybridizations. This is similar to the situation in bulk as found in experiment.[16] Therefore, the Zn vacancy prefers to reside on the nanowire surface, which results in a magnetic nanowire. The electronic structure of the nanowire bears some resemblance to that of the thin film surface. This can be seen from the total DOS and partial DOS of Zn and O atoms for configuration (b_3) plotted in Figs. 2(d)–2(f).

The origin of magnetism from O $2p$ orbitals, instead of Zn $3d$ orbitals, may have its roots in the atomic properties of oxygen. Note that the electronic configuration of O atom is $1s^2 2s^2 2p^4$ with two unpaired $2p$ electrons that lead to a moment of 2.0 μ_B. In O_2 molecules, there are also two unpaired electrons in the degenerate $2p$-π^* antibonding orbitals, so that the electronic ground state of O_2 is a spin triplet state. A monolayer O_2 on graphite also shows some interesting magnetic properties.[28] It is well known that solid O_2 in α phase is antiferromagnetic, and solid O_2 in β phase is a frustrated antiferromagnetic.[29,30] When O atom is substitutionally doped in solid of K, Rb, and Cs, the impurity O carries a magnetic moment of 0.870, 0.990, and 1.070 μ_B respectively.[31] When an O atom is placed in Li_{12}, Na_{12}, K_{12}, and Rb_{12} clusters with an icosahedral geometry, the O atom exhibits magnetic moments of 0.529, 1.216, 1.370, and 1.460 μ_B, respectively.[32] Similarly, a substitutionally doped O atom in BN sheet carries a magnetic moment of 1.0 μ_B.[33] Rb_4O_6 is found to be an intrinsic ferromagnet in which the magnetic moment is exclusively carried by the p electrons of O anions.[34]

Systems with magnetism based on $2p$ electrons are expected to display some novel properties not found in $3d$- or $4f$-electron systems. For example, valence electrons in p orbitals are more delocalized than those in d and f orbitals and the spin-orbit coupling is much smaller or negligible for atoms containing $2p$ valence electrons since it scales with the fourth power of the atomic number. Especially because the magnetism comes from O not from other d- or f-metal element, the system is more biocompatible for medicinal applications since metal atoms usually can induce the formation of some dangerous free radicals.

V. SUMMARY

In summary, using first-principles theory, we have systematically examined the electronic properties and magnetism of ZnO thin films and nanowires by using both Zn and O vacancies. We show that Zn vacancy introduces spin polarization of the top of the valence band and the observed magnetism in ZnO thin films arises indeed from Zn vacancies. These vacancies prefer to reside on the surface, as has been suggested from experiments. The origin of magnetism does not result from the Zn $3d$ electrons but from the unpaired $2p$ electrons of O atoms in the immediate vicinity of the Zn vacancies. Compared to thin films, it is not only easier to introduce Zn vacancy in ZnO nanowire, but the resulting magnetic moment is also larger. Our theoretical study confirms that one can have an alternative way to generate the low dimensional magnetic ZnO nanostructures by introducing Zn vacancies instead of doping with transition-metal

atoms. This provides us some advantages for biomedical applications (e.g., magnetic healing, oxygen delivery, improving biofluid circulation for effective transport and release, helping to bring a normal charge back to each body cell by increasing cellular oxygen, and restoring pH balances), as the absence of transition-metal atoms may prevent the formation of dangerous free radicals.

ACKNOWLEDGMENTS

The work was supported in part by grants from the U.S. Department of Energy. The authors thank the staff of the Center for Computational Materials Science, the Institute for Materials Research, Tohoku University (Japan), for their continuous support of the HITACH SR11000 supercomputing facility.

*sunq@coe.pku.edu.cn

[1] Koji Ando, Science **312**, 1883 (2006); U. Ozgur, Y. I. Alivov, C. Liu, A. Take, M. A. Reshchikov, S. Dogan, V. Avrutin, S. J. Cho, and H. Morkoc, J. Appl. Phys. **98**, 041301 (2005).
[2] A. Hausmann and B. Schallenberger, Z. Phys. B **31**, 269 (1978).
[3] A. Pöppl and G. Völkel, Phys. Status Solidi A **121**, 195 (1990).
[4] G. D. Mahan, J. Appl. Phys. **54**, 3825 (1983).
[5] G. Neumann, Phys. Status Solidi B **105**, 605 (1981).
[6] K. I. Hagemark, J. Solid State Chem. **16**, 293 (1976).
[7] S. F. J. Cox, E. A. Davis, S. P. Cottrell, P. J. C. King, J. S. Lord, J. M. Gil, H. V. Alberto, R. C. Vilao, J. Piroto Duarte, N. Ayresde Campos, A. Weidinger, R. L. Lichti, and S. J. C. Irvine, Phys. Rev. Lett. **86**, 2601 (2001).
[8] D. M. Hofmann, A. Hofstaetter, F. Leiter, H. Zhou, F. Henecker, B. K. Meyer, S. B. Orlinskii, J. Schmidt, and P. G. Baranov, Phys. Rev. Lett. **88**, 045504 (2002).
[9] F. Tuomisto, V. Ranki, K. Saarinen, and D. C. Look, Phys. Rev. Lett. **91**, 205502 (2003).
[10] A. Zubiaga, F. Tuomisto, F. Plazaola, K. Saarinen, J. A. Garcia, J. F. Rommeluere, J. Zuñiga-Pérez, and V. Muñoz-Sanjosé, Appl. Phys. Lett. **86**, 042103 (2005).
[11] G. Brauer, W. Anwand, W. Skorupa, J. Kuriplach, O. Melikhova, C. Misson, H. von Wenckstern, H. Schmidt, M. Lorenz, and M. Grundmann, Phys. Rev. B **74**, 045208 (2006).
[12] A. F. Kohan, G. Ceder, D. Morgan, and Chris G. Van de Walle, Phys. Rev. B **61**, 15019 (2001); A. Janotti and C. G. Van de Walle, J. Cryst. Growth **287**, 58 (2006).
[13] S. B. Zhang, S.-H. Wei, and Alex Zunger, Phys. Rev. B **63**, 075205 (2001).
[14] A. Uedono, T. Koida, A. Tsukazaki, and M. Kawasaki, J. Appl. Phys. **93**, 2481 (2003).
[15] Z. Q. Chen, S. Yamamoto, M. Maekawa, A. Kawasuso, X. L. Yuan, and T. SekiguchiJ. Appl. Phys. **94**, 4807 (2003).
[16] A. Zubiaga, F. Plazaola, J. A. Garcia, F. Tuomisto, V. Muñoz-Sanjosé, and R. Tena-Zaera, Phys. Rev. B **76**, 085202 (2007).
[17] N. H. Hong, J. Sakai, and V. Brize, J. Phys.: Condens. Matter **19**, 036219 (2007).
[18] W. Kohn and L. J. Sham, Phys. Rev. **140**, A1133 (1965).
[19] J. P. Perdew, K. Burke, and M. Ernzerhof, Phys. Rev. Lett. **77**, 3865 (1996).
[20] Y. Wang and J. P. Perdew, Phys. Rev. B **44**, 13298 (1991).
[21] G. Kresse and D. Joubert, Phys. Rev. B **59**, 1758 (1999).
[22] G. Kresse and J. Furthmüller, Phys. Rev. B **54**, 11169 (1996).
[23] Q. Wang and P. Jena, Appl. Phys. Lett. **84**, 4170 (2004).
[24] Q. Wang, Q. Sun, P. Jena, and Y. Kawazoe, Appl. Phys. Lett. **87**, 162509 (2005); Q. Wang, Q. Sun, B. K. Rao, and P. Jena, Phys. Rev. B **69**, 233310 (2004).
[25] A. Janotti and C. G. Van de Walle, Phys. Rev. B **76**, 165202 (2007).
[26] F. Tuomisto, K. Saarinren, D. C. Look, and G. C. Farlow, Phys. Rev. B **72**, 085206 (2005).
[27] J. Monkhorst and J. D. Pack, Phys. Rev. B **13**, 5188 (1976).
[28] J. P. Mctague and M. Nielsen, Phys. Rev. Lett. **37**, 596 (1976).
[29] P. W. Stephens and C. F. Majkrzak, Phys. Rev. B **33**, 1 (1986).
[30] R. J. Meier and R. B. Helmholdt, Phys. Rev. B **29**, 1387 (1984).
[31] N. Papanikolaou, N. Stefanou, R. Zeller, and P. H. Dederichs, Phys. Rev. Lett. **71**, 629 (1993).
[32] Q. Sun, Q. wang, and S.-Y. Wang, Phys. Lett. A **228**, 297 (1997).
[33] R.-F. Liu and C. Cheng, Phys. Rev. B **76**, 014405 (2007).
[34] J. J. Attema, G. A. de Wijs, G. R. Blake, and R. A. de Groot, J. Am. Chem. Soc. **127**, 16325 (2005).